Appl Biochem Biotechnol (2009) 158:631–641
DOI 10.1007/s12010-008-8348-3

Characterization of the Interactions of Lysozyme with DNA by Surface Plasmon Resonance and Circular Dichroism Spectroscopy

Kuo-Chih Lin · Ming-Tsai Wey · Lou-Sing Kan · David Shiuan

Received: 26 June 2008 / Accepted: 18 August 2008 /
Published online: 2 October 2008

Abstract Association with nucleic acid has been recognized as a unique role of lysozyme and may explain why lysozyme was called a killer protein against HIV infection. In the present study, we characterized the interactions of lysozyme and its derived peptides with a biotin-labeled pUC19 plasmid DNA. Real-time detection of the macromolecular interaction was performed using the SPR (surface plasmon resonance) spectroscopy. The SPR sensorgrams were analyzed and the association and dissociation rate constants as well as the dissociation equilibrium constant K_D were, thus, estimated. The results reveal that other than the electrostatic interactions between the basic protein and the nucleotide sequences carrying negative charges, the specific DNA-binding motifs at the N- and C-termini of lysozyme were also involved in the interactions. The nonapeptide RAWVAWRNR (aa 107–115 of lysozyme) reported previously to block HIV-1 viral entrance and replication was also able to bind DNA with its K_D value comparable to that of histones. The possibilities of ligand-binding-induced conformational changes were investigated using the circular dichroism spectroscopy. The CD spectra (200–320 nm) reveal that the conformational changes indeed occur as the spectra of lysozyme–DNA interactions are much less at the major trough region than the sum of individual spectra. The interaction of lysozyme with DNA molecules may interfere with DNA replication, modulate gene expression, and block bacterial and viral infections. These all suggest that human lysozyme may represent part of the innate immune system with a very broad protective spectrum.

Keywords Circular dichroism spectroscopy · Dissociation equilibrium constant · DNA · Lysozyme · Molecular interaction · Surface plasmon resonance

K.-C. Lin · D. Shiuan (✉)
Department of Life Science, Institute of Biotechnology and the Bioinformatic Program, National Dong Hwa University, Hualien, Taiwan 974, Republic of China
e-mail: shiuan@mail.ndhu.edu.tw

M.-T. Wey
College of Life Science, National Tsinghua University, Hsinchu 300, Taiwan

M.-T. Wey · L.-S. Kan
Institute of Chemistry, Academia Sinica, Taipei, Taiwan 112, Republic of China

Abbreviation

CD spectroscopy	circular dichroism spectroscopy
HEW	hen egg-white
SPR	surface plasmon resonance

Introduction

Lysozyme is an abundant, antimicrobial protein widely distributed in nature. It has been found in mammalian tissues and secretions, bacteria, virus, insects, and plants [1]. Lysozyme is well known for its muramidase activity which hydrolyzes the bond between *N*-acetylglucosoamine and *N*-acetyl muramic acid leading to degradation of peptidylglycan in the cell wall of Gram-positive bacteria. In addition, lysozyme has also been reported to have functions including the induction of fusion of phospholipid vesicles [2], DNA-membrane association [3], antitumor activities [4], inhibition of HIV replication [5], and association with nucleic acids [6].

In mammals, lysozyme is produced by the cytoplasmic granules of most cells and is present in all body fluids and blood at 0.5–2.0 mg/ml [7]. Lysozyme is a unique protein which has a small compact globular structure with a net positive charge at physiological pH. For example, hen egg-white (HEW) lysozyme [8] has 19 positive charged amino acid residues (4K, 1H, 14R) and the p*I* is 10.7. The bactericidal action of lysozyme is intensive to Gram-positive bacteria but much weaker to Gram-negative bacteria. The differential activities of lysozyme have attracted the efforts to elucidate its detailed action mechanisms. The findings that denaturation of lysozyme by heat or dithiothreitol did not abolish its bactericidal activity led to the suggestion that the bactericidal activity of lysozyme was not only due to the muramidase activity [9]. Further study indicates that the insertion of a hydrophobic pentapeptide into the C-terminus of lysozyme can enhance the bactericidal action toward *E. coli* [10]. More striking evidence comes from the finding that the pentapeptide (corresponding to the amino acids 98–112 of HEW lysozyme) generated from fractionation of clostripain-digested lysozyme has antimicrobial activity but without muramidase activity [11, 12]. Lately, the mutation abolishes the catalytic activity of lysozyme but retains its antimicrobial activity further demonstrates that the antimicrobial capability is independent of the muramidase activity [13]. However, despite the huge efforts, the biological importance of lysozyme in host defense and the action mechanism are still not completely understood.

In addition to the enzyme activity, the association with nucleic acid has been recognized as a unique role of lysozyme and may explain why lysozyme was called a killer protein against HIV infection [5, 6]. A recent study reveals that even a short nonapeptide HL9 (part of lysozyme) has the antiviral activity [14]. However, the antiviral activity can not be fully explained by the basicity or the secondary structure of HL9, and there is no clue about the presence of HL9 and HL18 in vivo [14]. We, therefore, set forth to characterize the interactions of lysozyme and its derived peptides with DNA molecules and to examine if the binding may induce conformational changes of DNA and lysozyme. The recent availability of optical biosensors, such as surface plasmon resonance (SPR) spectroscopy, allows us for real-time detection of the macromolecular interactions and the determination of binding kinetics and affinities [15–17]. In this study, the bindings of lysozyme and its derived peptides with DNA molecules with lysozyme and its derived peptides were measured by SPR spectroscopy. The possibilities of pUC19 binding-induced conformational changes were also investigated using the circular dichroism spectroscopy.

Materials and Methods

Materials

HEW lysozyme (NCBI accession number NP_990612) and human lysozyme (NCBI accession number CAA32175) were purchased from Sigma (USA). The amino acid sequence of human lysozyme is N′-KVFERCELARTLKRLGMDGYRGISLA NWMC LAKWESGY NTRAT NYNAGDRSTDYGIFQINSRYWCNDGKTPGAVNACHLSCS ALLQDNIADAVACAK RVVRD PQGIRAWVAWRNRCQNRDVRQ YVQGCGV-C′, with the helix–turn–helix motifs underlined. The human lysozyme-derived peptides A40 (40 aa long, containing the N-terminal helix–turn–helix motif; N′-KVFERCELARTLKRLGMDGYRGISLA NWMCLAKWE SGYNT-C′); B40 (40 aa long, containing the C-terminal α-helix and HL9; N′-CSALLQDNIADAVACAKRVV RDPQGIRAWVAWR NRCQNRD-C′); and C9 (9 aa long, containing only the HL9, N′-RAWVA WRNR-C′) were synthesized, purified by FPLC and verified by mass spectrum by Kelowna Scientific Co. (Taipei, Taiwan).

Plasmid pUC19 DNA was purchased from Sigma (USA) and then prepared from a transformed *E. coli* strain using the alkaline method. The double-stranded biotinylated pUC19 was generated by PCR using the biotin-labeled primers located adjacent to the ends of multiple cloning site of pUC19 and the DNA of plasmid pUC19 as the template. The biotin-labeled primers F30 and R30 (forward primer F30: 5′-biotin-ctggccgtcg ttttacaacg tcgtgactgg-3′ and the reverse primer R30: 5′-biotin-gttatccgct cacaattcca cacaacatac-3′) were synthesized and purified by HPLC by MDBio Inc. (Taipei, Taiwan). In the study, lysozyme, peptides, and DNAs were dissolved in PBS buffer (137 mM NaCl, 8 mMNa_2HPO_4, 1.5 mM KH_2PO_4 and 2.7 mM KCl, pH7.53). The high ionic strength of the buffer should be able to minimize the long-range electrostatic interactions between lysozyme and DNA molecules. Restriction enzyme *Eco*RI used to linearize the plasmid pUC19 was obtained from New England Biolab (USA).

SPR (Surface Plasmon Resonance) Measurements

SPR measurements were performed using a BIAcore 3000 system and a sensor chip SA (BIAcore, Uppsala, Sweden). The SA sensor chip consists of a gold surface to which a carboxymethylated dextran layer is bound. The dextran layer is activated with streptavidin by the manufacturer. Prior to the experiment, the streptavidin surface was cleaned three times with the regeneration buffer (50 mM NaOH in 1 M NaCl) and equilibrated with the PBS buffer before DNA immobilization. Biotinylated plasmid pUC19 (40 μL, 30 nM) was injected to a single flow cell at a flow rate of 10 μL/min and immobilized. Once the pUC19-biotin-coated sensor chip was stable in the running buffer (PBS, flow rate 10 μL/min), lysozyme or the derived peptides (in PBS) was injected over the surface at various concentrations at a flow rate of 10 μL/min. Each sample was separated by an interval of 3 min and the regeneration process was carried out by injection of 30 μL regeneration buffer. All buffer solutions were filtered (0.2 μm filter) and deoxygenated. Repeated experiments indicated that the regeneration procedure did not change the binding characteristics of ligand DNAs. The sensorgrams were analyzed by the global fitting procedure using a 1:1 (Langmuir type) drifting baseline model-derived equation [18] available in the BIA evaluation 3.0 software (*BIAevaluation 3.0 Software Handbook*, 1997). We chose the sensorgrams that appeared approximately at the 10–30-s periods after the association and the dissociation processes to fit in the model. All of the measurements were repeated at least three times. The association rate constant k_a and the dissociation rate

constant k_d as well as the dissociation equilibrium constants K_D were estimated when the Chi^2 values were minimized.

CD (Circular Dichroism) Spectral Analysis

The CD spectra were measured using a Jasco J-815 spectropolarimeter (Japan Spectroscopic Co., Japan) equipped with a temperature control unit (PTC-423S/15). Circular dichroism was expressed as the difference in the molar absorption of the left- and right-handed circularly polarized light, in the units of M^{-1} cm^{-1}. The spectra were scanned in the range of 200–320 nm in a 500-L cell with a 1-mm pathlength. The spectra shown were the accumulated averages of three scans, each recorded at a scan rate of 1.0 nm/s. The protein and DNA samples were also prepared in PBS solution (pH 7.53).

Results

Association with nucleic acid has been recognized as a unique role of lysozyme and may help to explain the wide-spread antimicrobial effects of lysozyme. Based on the gel electrophoresis data, both human lysozyme and HEW lysozyme have been demonstrated to bind DNA equally well [6]. Therefore, we decided to use HEW lysozyme and the human lysozyme-derived peptides, A40 and B40, that contain the DNA-binding motif to monitor their interactions with a biotin-labeled pUC19 plasmid DNA (and its derived F30 oligonucleotide) using the SPR measurements. The amino acid sequences of human lysozyme and chicken egg-white lysozyme were aligned and compared with BLAST algorithm [19]. As shown in Fig. 1, the comparison showed 60% identities and 78% positive (with the "+" symbols) between the two sequences. To perform the experiments, the biotin-labeled pUC19 plasmid DNA was first immobilized on the surface of SA chip which was coated with streptavidin. As shown in Fig. 2a, the binding of biotin-labeled pUC19 plasmid DNA causes an increase of approximately 600 RU (resonance units) at the sensorgram and the DNA was stably maintained on the chip. The protein and peptide samples were then injected and flowed through the channels on the chip and interacted with the bound pUC19 DNA. The sensorgrams were typified by an abrupt shot followed by a steady increase until the plateau was reached. The concentrations of lysozyme and peptides were usually adjusted to the range of 4 to 256 μM (such as 3.9; 7.8; 15.6; 31.3; 62.5, and 125 μM) so that the changes of resonance units were in the range of 50 to 1,000 RU. As shown in Fig. 2b and c, the association sensorgram of each sample was recorded for 4 min and the dissociation process (washed by PBS buffer) for another 4 min. To remove the bound lysozyme or peptides, the chip was regenerated by the injection of 30 μL regeneration buffer which caused a very high RU change between the measurements. Repeated experiments indicated that the regeneration procedure did wash away the bound lysozyme, returned to the baseline and did not change the binding characteristics of biotin-labeled pUC19. As shown in Fig. 2c, the sensorgrams of the interactions of the pUC19-biotin DNA with lysozyme of various concentrations were aligned. Again, the aligned sensorgrams exhibited an abrupt rise followed by a slower phase and then climbed up the plateau. Similarly, in the dissociation process, a quick drop was followed by the slower path and gradually returned to a new baseline before the injection of regeneration buffer. The aligned SPR sensorgrams were then analyzed and the association and dissociation rate constants were thus estimated [18]. The interactions of biotin-labeled pUC19 on the SA chip with lysozyme, peptide A40, peptide B40, and peptide C9 were assayed and analyzed

```
Human  1
KVFERCELARTLKRLGMDGYRGISLANWMCLAKWESGYNTRATNYNAGDRSTDYGIFQIN  60
            KVF RCELA  +KR G+D YRG SL NW+C+AK+ES +NT+ATN N  D STDYGI QIN
Chick  19
KVFGRCELAAAMKRHGLDNYRGYSLGNWVCVAKFESNFNTQATNRNT-DGSTDYGILQIN  77

Human  61
SRYWCNDGKTPGAVNACHLSCSALLQDNIADAVACAKRVVRDPQGIRAWVAWRNRCQNRD  120
            SR+WCNDG+TPG+ N C++ CSALL  +I  +V CAK++V D  G+ AWVAWRNRC+  D
Chick  78
SRWWCNDGRTPGSRNLCNIPCSALLSSDITASVNCAKKIVSDGNGMSAWVAWRNRCKGTD  137

Human  121  VRQYVQGC  128
             V+ +++GC
Chick  138  VQAWIRGC  145
```

A40: N'-KVFERCELARTLKRLGMDGYRGISLANWMCLAKWE SGYNT-C'

B40: N'-CSALLQDNIADAVACAKRVVRDPQGIRAWVAW NRCQNRD-C'

C9: N'-RAWVAWRNR-C'

Fig. 1 The BLAST comparison of human lysozyme and chicken egg-white lysozyme. The human lysozyme has 130 amino acids while the HEW lysozyme has 147 amino acids. The 18 amino acids at the N-terminal are the signal peptides. The "+" symbols represent the positive charged regions where the physical nature of amino acid residues are the same. The *underlined regions* represent the peptide A40 at the N-terminus, and the peptide B40 at the C-terminus. The peptide C9 locates at the C-terminal end of peptide B40

similarly. As shown in Table 1, the K_D values of lysozyme and the derived peptides interacted with pUC19 all fell in the range of 10^{-4} to 10^{-6} M. Even the short nonapeptide, C9, which has been reported previously to block HIV-1 viral entrance and replication, was able to bind with DNA reasonably well. The K_D values of pUC19-lysozyme and pUC19-peptide, A40, are comparable. In contrast, the pUC19-peptide, B40, exhibited a much higher dissociation constant. The approximately 30-fold difference between the K_D of the pUC19-peptide, A40, and the K_D of the pUC19-peptide, B40, could be due to the two-fold difference in k_d and the approximately 60-fold difference in k_a.

The possibilities of pUC19-binding-induced conformational changes were investigated using the circular dichroism spectroscopy. As shown in Fig. 3a and b, the CD spectra of the B-form pUC19 exhibit almost no change from 25°C to 75°C while the concentration dependence (15–125 nM) spectra reveal several changes including a peak band at 270 nm and two troughs (negative bands) at 210 and 245 nm. The CD spectra of lysozyme were characterized by a simple negative band near 210 nm and a much weaker trough near 225 nm. As the temperature elevated to 65°C, the trough of the spectra tended to have a blue shift and the size reduced as shown in Fig. 3c. The CD spectra of lysozyme exhibited a rather simple concentration-dependent manner without changing the spectra shape from 3.125 to 50 μM (Fig. 3d). The CD spectra of peptide B40 (10 μM) and C9 (10 μM) were

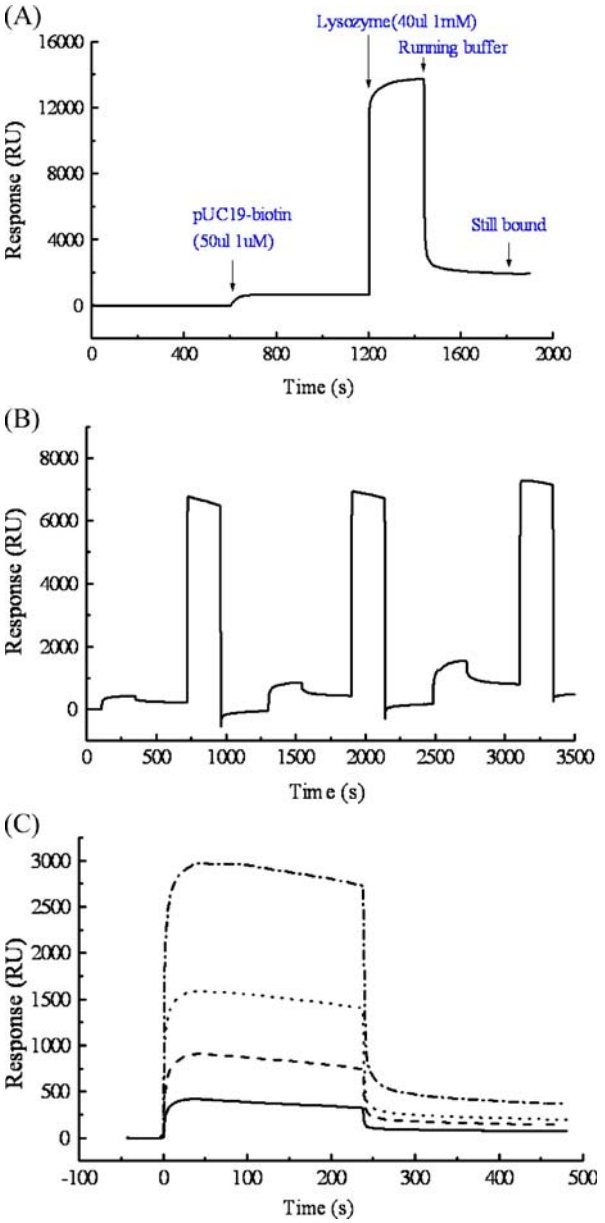

Fig. 2 The SPR sensorgrams were measured to monitor the interaction of lysozyme and its derived peptides with the biotin-labeled pUC19 and F30 at 25°C. **a** The sensorgram showing that the biotin-labeled pUC19 was coated onto the SA chip. **b** The SPR sensorgrams were measured with peptide B40 of varied concentrations flowing through the channels and detected during the interactions. Peptide B40 additions of 7.81 μM (100–500 s), 15.6 μM (1,300–1,700 s), and 31.3 μM (2,500–1900 s). **c** The sensorgrams the pUC19-biotin DNA with lysozyme of various concentrations (from top: 0.97 μM, 7.81 μM, 15.6 μM, 31.3 μM) were aligned for further kinetics analysis

also measured. As shown in Fig. 3e, the negative band of the CD spectrum of the peptide B40 was shifted to 207 nm and the size reduced as compared with lysozyme of similar concentration. However, the C9 spectrum was much sharper and the trough shifted further to 204 nm. The CD spectra of lysozyme–DNA interactions were also measured. As shown in Fig. 3f, the spectra of pUC19 (30 nM), lysozyme (5 μM) and the mixture of pUC19 with lysozyme were displayed. Comparing with the lysozyme spectrum, the spectrum of the mixture remained almost the same except that it had a shoulder at 270 nm, a small negative

Table 1 Rate constants (k_a, k_d) and dissociation constant K_D (mean±standard deviation) for the interaction between lysozyme (and its derived peptides) with DNA.

Interaction	$k_a \times 10^2$ ($M^{-1}s^{-1}$)	$k_d \times 10^{-2}$ (s^{-1})	$K_D \times 10^{-5}$ (M)	Chi^2
F30-lysozyme	5.73±0.49	8.09±1.08	14.1±1.22	49.3
pUC19-lysozyme	21.04±1.88	1.09±0.08	0.52±0.03	84
pUC19-A40	88.62±9.25	3.49±0.55	0.39±0.03	1.81
pUC19-B40	1.30±0.09	1.71±0.20	13.2±1.27	2.45
pUC19-C9	13.7±1.52	3.21±0.03	2.35±0.31	1.99

band at 245 nm, and a little rise near 220 nm. Obviously, the spectrum of the mixture is quite different from the calculated spectrum which is the summation of the two individual spectra. Similar findings were also observed for the spectra of pUC19 (30 nM), lysozyme (3 μM), and the mixture at 25°C and 75°C as well (data not shown).

Discussion

The present study has demonstrated that lysozyme and its derived peptides bind with plasmid DNA effectively (Fig. 2 and Table 1). The sensorgrams were typified by a sharp rise followed by a steady increase until the plateau was reached. Similarly, in the dissociation process, a quick drop was followed by a slower path and gradually returned to a new baseline before the injection of regeneration buffer. We speculate that the initial abrupt changes during the association and dissociation phases appeared on the sensorgrams were due to the strong short-range electrostatic interactions between the positively charged lysozyme (and its derived peptides) with the negatively charged DNA molecules. The diffusion-limited process was followed by the formation of docking complex while the salt bridges and H-bonds may play equal roles. In the present study, we found that even the short nonapeptide, C9 (aa 107–115 of lysozyme), which had been reported previously to block HIV-1 viral entrance and replication [5], was able to bind with DNA reasonably well. Therefore, other than the electrostatic interactions between the basic protein and the nucleotide sequences carrying negative charges, the specific DNA-binding motifs at the N- and C-termini of lysozyme must have also involved in the interactions. Aside from the pure charge effects, the sensorgrams of the later phase (10–30 s after the mixing) representing the real molecular interactions between the proteins and plasmid DNA were chosen for further sensorgram analysis. The dissociation constant K_Ds of lysozyme, peptides A40, B40, and C9 with plasmid DNA were estimated to be in the range of 10^{-4} to 10^{-6} (Table 1). These values are comparable to the bindings of histones toward chromosomal DNAs [20], the serum factor to the DNA containing specific binding site [21] and the temperate P2-like bacteriophage repressors toward their operator sequences [22]. The most striking finding is that the K_D value (2.35×10^{-5} M) of the nonapeptide, C9, is very close to that of the histones [20]. However, it is really difficult to explain the approximately 30-fold difference between the K_D of the peptide A40 and peptide B40. Both peptide A40 and peptide B40 contain a helix–turn–helix DNA-binding motif and six positively charged amino acids. The relatively high values in k_a (13.7×10^{-2} M^{-1} s^{-1}) and K_D (2.35×10^{-5} M) of the C-termini nonapeptide C9 may explain partially the unusually high K_D value of peptide B40.

The conformational changes of nucleic acids such as the conformational transition from B form to A form are difficult to follow, though the CD spectrum of the A-form DNA was dominated by a strong positive band close to 270 nm [23]. The CD spectra of the mixture of

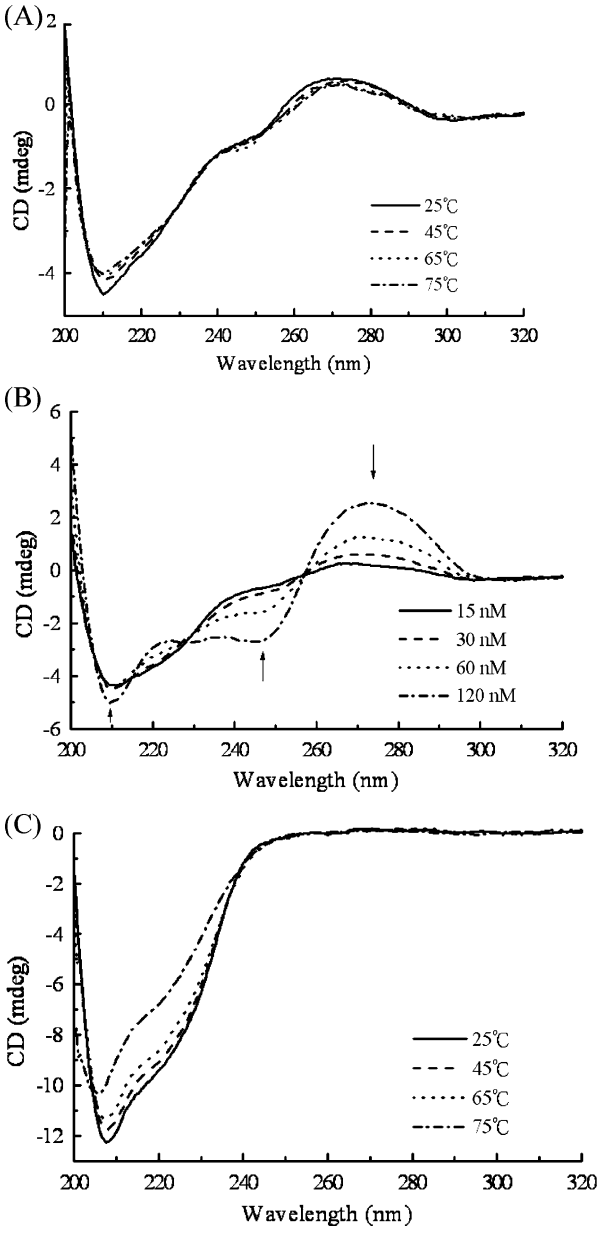

Fig. 3 The CD spectra of pUC19, lysozyme, peptide C9, B40 and the interactions of lysozyme with pUC19 DNA. **a** Temperature dependence of the CD spectra of pUC19 at 25, 45, 65, and 75°C. **b** Concentration dependence of the CD spectra of pUC19 at 15, 30, 60, and 120 nM at 25°C. **c** Temperature dependence of the CD spectra of lysozyme at 25, 45, 65, and 75°C. **d** Concentration dependence of the CD spectra of lysozyme at 3.125, 6.25, 12.5, 25, and 50 μM. **e** The CD spectra of peptide C9 (10 μM) and B40 (10 μM) at 25°C. **f** The spectra of pUC19 (30 nM), lysozyme (5 μM) and the mixture (30 nM pUC19 and 5 μM lysozyme)

lysozyme and DNA are always less than that of the calculated spectra of the individuals at 25°C (and also at 75°C, data not shown), revealing that the secondary structures of lysozyme and pUC19 were changed upon interactions. This is in accordance with the postulation that ligand binding often induces conformational changes in both the receptor and ligand during the docking step [24]. However, whether the conformation of lysozyme or pUC19 or both were changed during the protein–DNA interactions was not resolved with the present CD study. The possibilities of forming an aggregated complex and the

Fig. 3 (continued)

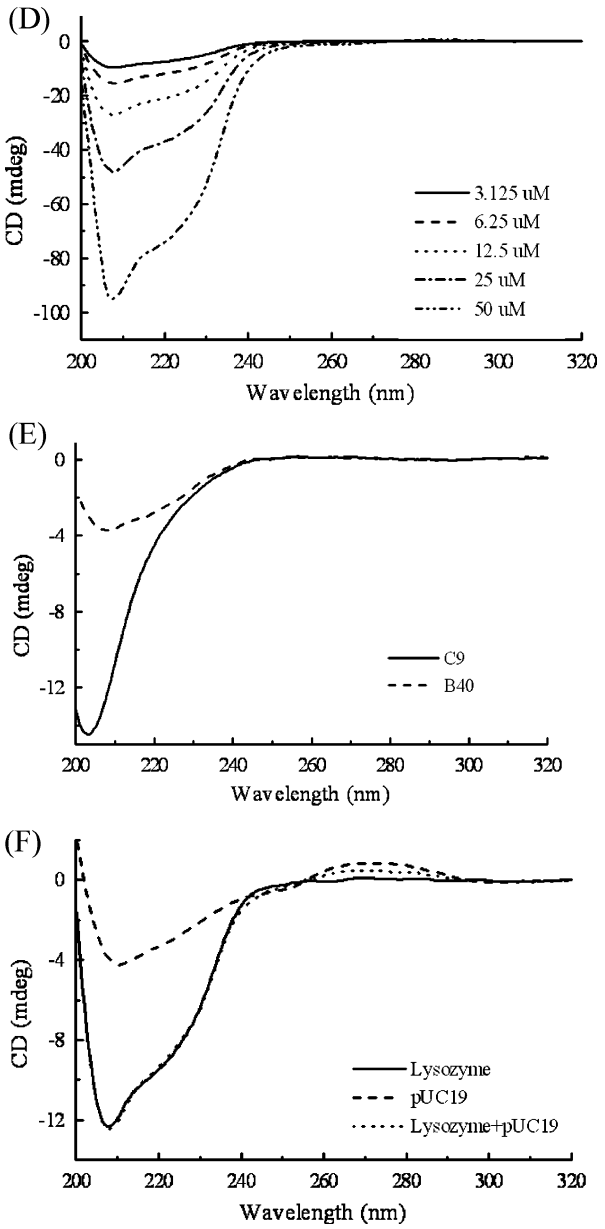

sizes of the binding complexes in a colloidal state await further investigations using the dynamic laser light scattering system.

Lysozyme contains a C-terminal motif with α-helix and positive charge (aa 88–115, within the peptide B40) which is commonly found in bactericidal and the cell-penetrating peptides [25]. In fact, the human lysozyme, HEW lysozyme, and their corresponding C-terminal peptides (aa 88–115) and the nonapeptides (aa107–114) were reported to permeabilize the outer membrane and inner membrane of *E. coli* [26]. However, to the

best of knowledge, no report has even suggested that lysozyme was cleaved in eukaryotic cells to generate such nonapeptides [14]. The present study has characterized the interactions between lysozyme and DNA molecules through SPR and CD experiments. The reasonably strong bindings of lysozyme and its derived peptides with DNA molecules have provided an alternative explanation for the antimicrobial capabilities of lysozyme and its derived peptides. This all suggests that human lysozyme may represent part of the innate immune system with a very broad protective spectrum.

Acknowledgement The present work was supported in part by the grants (NSC95-2113-M001-043 to LSK; NSC94-2311-B259-005 to DS) from National Science Council, ROC. The authors also thank Academia Sinica for providing the research supporting grant (Academia Sinica 72v112) for visiting scholars (to DS).

Reference

1. Schindler, M., Assaf, Y., Sharon, N. D., & Chipman, M. (1977). *Biochemistry*, *16*, 423–431. doi:10.1021/bi00622a013.
2. Posse, E., DeArcuri, B. F., & Morero, R. D. (1994). *Biochimica et Biophysica Acta*, *1193*, 101–106. doi:10.1016/0005-2736(94)90338-7.
3. Siberstein, S., & Inouye, M. (1974). *Biochimica et Biophysica Acta*, *366*, 149–158.
4. Sava, G., Ceschia, V., & Zabucchi, G. (1988). *European Journal of Cancer & Clinical Oncology*, *24*, 1737–1743. doi:10.1016/0277-5379(88)90075-2.
5. Lee-Huang, S., Huang, P. L., Sun, Y., Kung, H. F., Blithe, D. L., & Chen, H. C. (1999). *Proceedings of the National Academy of Sciences of the United States of America*, *96*, 2678–2781. doi:10.1073/pnas.96.6.2678.
6. Steinrauf, L. K., Shiuan, D., Yang, W. J., & Chiang, M. Y. (1999). *Biochemical and Biophysical Research Communications*, *266*, 366–370. doi:10.1006/bbrc.1999.1804.
7. Jolles, P. (1996). *EXS*, *75*, 3–5.
8. Dickerson, R. E., Reddy, J. M., Pinkerton, M., & Steinrauf, L. K. (1962). *Nature*, *196*, 1178. doi:10.1038/1961178a0.
9. Pellegrini, A., Thomas, U., von Fellenberg, R., & Wild, P. (1992). *The Journal of Applied Bacteriology*, *72*, 180–187.
10. Ibrahim, H. R., Yamada, M., Kobayashi, K., & Kato, A. (1992). *Bioscience, Biotechnology, and Biochemistry*, *56*, 1361–1363.
11. Pellegrini, A., Bramaz, T. N., Klauser, S., Hunziker, P., & von Fellenberg, R. (1997). *Journal of Applied Microbiology*, *82*, 372–378. doi:10.1046/j.1365-2672.1997.00372.x.
12. During, K., Porsch, P., Mahn, A., Brinkmann, O., & Gieffers, W. (1999). *FEBS Letters*, *449*, 93–100. doi:10.1016/S0014-5793(99)00405-6.
13. Ibrahim, H. R., Matsuzaki, T., & Aoki, T. (2001). *FEBS Letters*, *506*, 27–32. doi:10.1016/S0014-5793(01)02872-1.
14. Lee-Huang, S., Maiorov, V., Huang, P. L., Ng, A., Lee, H. C., Chang, Y. T., et al. (2005). *Biochemistry*, *44*, 4648–4655. doi:10.1021/bi0477081.
15. Wu, S. J., & Chailen, I. (2004). *Methods in Molecular Biology (Clifton, N.J.)*, *249*, 93–110.
16. Schubert, H., Zettl, W., Hafner, G., & Krausch, G. (2003). *Biochemistry*, *42*, 10288–10294. doi:10.1021/bi034033d.
17. Stenlund, P. G., Babcock, J., Sodroski, J., & Myszka, D. G. (2003). *Analytical Biochemistry*, *316*, 243–250. doi:10.1016/S0003-2697(03)00046-0.
18. Kobayashi, Y., Nakamura, H., Sekiguchi, T., Takanami, R., Murata, T., Usui, T., et al. (2005). *Analytical Biochemistry*, *336*, 87–93. doi:10.1016/j.ab.2004.09.029.
19. Schaffer, A. A., Aravind, L., Madden, T. L., Shavirin, S., Spouge, J. L., Wolf, Y. I., et al. (2001). *Nucleic Acids Research*, *29*, 2994–3005. doi:10.1093/nar/29.14.2994.
20. Oohara, I., & Wada, A. (1987). *Journal of Molecular Biology*, *196*, 389–397. doi:10.1016/0022-2836(87)90699-1.
21. Singhal, R. P., & Otim, O. (2000). *Biochemical and Biophysical Research Communications*, *272*, 251–258. doi:10.1006/bbrc.2000.2720.
22. Henriksson-Peltola, P., Sehlen, W., & Haggard-Ljungquist, E. (2007). *Nucleic Acids Research*, *35*, 3181–3191. doi:10.1093/nar/gkm172.

23. Nejedly, K., Chladkova, J., Vorlickova, M., Hrabcova, I., & Kypr, J. (2005). *Nucleic Acids Research*, *33*, e5. doi:10.1093/nar/gni008.
24. Lindner, A. B., Eshhar, Z., & Tawfik, D. S. (1999). *Journal of Molecular Biology*, *285*, 421–430. doi:10.1006/jmbi.1998.2309.
25. Srisailam, S., Arunkumar, A. I., Wang, W., Yu, C., & Chen, H. M. (2000). *Biochimica et Biophysica Acta*, *1479*, 275–285.
26. Ibrahim, H. R., Thomas, U., & Pellegrini, A. (2001). *The Journal of Biological Chemistry*, *47*, 43767–43774. doi:10.1074/jbc.M106317200.